31st International Conference
ENGINEERING MECHANICS 2025
Medlov, Czech Republic, May 12 –14, 2025
Paper **#53**, pp. 193–196, doi: 10.21495/em2025-193

DIGITAL TWIN OF INDUSTRIAL BUILDING FOR TUNED MASS DAMPER APPROPRIATE DESIGN

Sokol M.[1], Mazáčková K.[1], Venglár M.[1], Crespo-Sanchez S.[2]

Abstract: *A new industrial building was constructed for processing rough mining material, with sieves used for rock sorting. However, these sieves induced intense dynamic effects, resulting in significant vibrations. The building's design did not incorporate dynamic assessments, leading to unbearable vibrations that severely restricted its operation. To address this issue, dynamic measurements were conducted to determine the building's parameters and its resulting dynamic response. As a solution, a tuned mass damper (TMD) was designed for the building's critical parts. The TMD parameters were optimized, and its performance was validated through extensive dynamic numerical analyses. Samples of these dampers were fabricated in the laboratory and subsequently installed in the building. The effectiveness of the dampers was evaluated through both numerical analysis and in-situ tests. These procedures demonstrated that the numerical model, developed using the Finite Element Method (FEM), accurately represents the system as a digital twin, including the building, dynamic drivers, and tuned mass dampers.*

Keywords: Tuned mass damper, digital twin, time history analysis, dynamic tests

1. Numerical model of the industrial building

For improved control and analysis of the measurement results, a reference FEM model was developed based on the provided project documentation. This model primarily consists of a beam structure (Fig. 1), where the columns are represented by steel cross-sections of type HEA 160, 220. The floor beams are modeled using IPE 220 type cross-sections. The stiffeners are represented as square hollow sections (SHS), with dimensions ranging from 160/160 and a wall thickness of 5 mm, to 220/220 with a wall thickness of 8 mm.

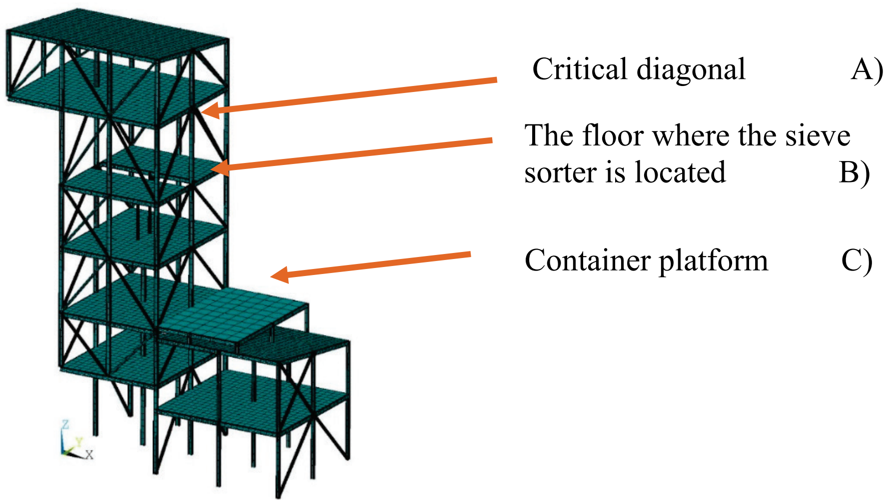

a) b)

Fig. 1: A) FEM model of the structure b) description of critical parts.

The floor slabs were modeled using planar elements to accurately represent their function as floor diaphragms. Their shear stiffness was designed to be equivalent to that of a more complex floor structure,

---

[1] Milan Sokol, Karolína Mazáčková, Michal Venglár, Slovenská University of Technology in Bratislava, Radlinského 11, 810 05 Bratislava, SK milan.sokol@stuba.sk, xmazackova@stuba.sk, michal.venglar@stuba.sk
[2] Saul Crespo-Sánchez, Tecnológico de Monterrey, Campus Querétaro, Mexico, secrespo@tec.mx

which consists of steel beams and trapezoidal sheets with overcasting. Figure 2 illustrates the significant eigenfrequencies and eigenmodes, which describe both global (a) to d) and some local (e) and f) vibrations.

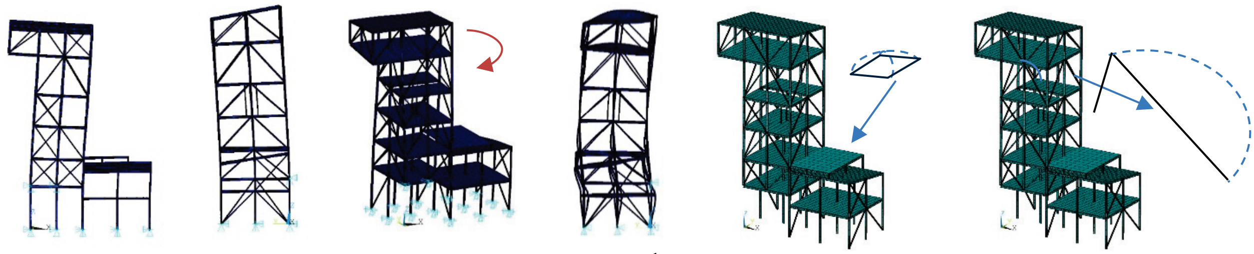

a) x-axis 1st b) y-axis 1st c) torsion 1st d) y-axis 2nd e) container platform f) critical diagonal

Fig. 2: Significant eigen frequencies and modes, a) 1,6Hz, b) 2,1Hz, c) 3,9Hz, d) 6,6Hz, e)5.9 Hz f) 13Hz

2. Test results and FEM model calibration

The results of the gradually calibrated FEM model for eigenfrequencies and eigenmodes are presented in Tab. 1, illustrating the model tuning process. Finally, it was necessary to account for all secondary structural components, such as conveyor belts, machines installed on specific platforms, etc. After incorporating these elements, the measured and calculated eigenfrequencies and eigenmodes showed a strong correlation.

Tab. 1: Process of preparing the appropriate digital twin with respect to eigen frequencies matching

Calibration steps		1. Freq (Hz)	2. Freq (Hz)	3. Freq (Hz)	5. Freq (Hz)
	FEM analysis				
1	Without conveyors belt	1,55	2,08	3,90	6,58
2	With vertical conveyor belt	2,42	2,62	4,43	6,66
3	With horizontal conveyor belt	1,57	2,23	4,00	6,65
4	With all secondary structures	**2,47**	**2,76**	**4,48**	**6,71**
	TEST results				
	Global frequencies	**2,31**	**2,85**	**4,11**	**7,01**

As a result of this calibration, a reliable digital twin of the structure was established. With this model, it became relatively straightforward to determine the appropriate values for the damping device (TMD) that could effectively reduce the vibrations (Clough and Penzien, 1993).

3. Tuned mass damper parameters

An overview of typical damping devices is provided by Sarwar and Sarwar (2019). The numerical scheme of the TMD is illustrated in Fig. 3.

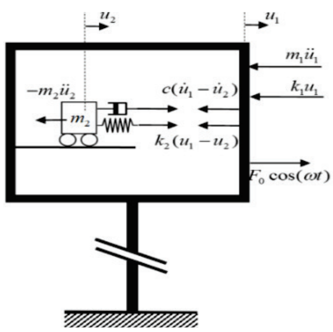

Fig. 3: TMD scheme

The system consists of a mass m_2 connected to the main structure by a spring k_2 and a damper c. The values of these components must be carefully selected to ensure the TMD's efficiency across a wide frequency range. The design of the TMD for the container platform (Fig. 1) is further discussed. In this case, the main system is modeled as a Single Degree of Freedom (SDOF) system, with mass m_1 and stiffness k_1 representing the container platform, and experiencing vertical displacement u_1 due to harmonic excitation at resonance *F₀cos(ωt)*. The damping of the platform is neglected, meaning $c_1 = 0$. The damping constant ccc of the TMD must be determined. The added mass m_2 is connected to the structure through a spring k_2 and a damper c, with displacement u_2. By solving the two differential equations governing the system, the dynamic response of both the main system and the TMD can be found (Pacht and Flesch, 1993).

$$m_1\ddot{u}_1 + c(\dot{u}_1 - \dot{u}_2) + k_1 u_1 + k_2(u_1 - u_2) = F_0 \cos \omega t \tag{1}$$

$$m_2\ddot{u}_2 + c(\dot{u}_2 - \dot{u}_1) + k_2(u_2 - u_1) = 0 \tag{2}$$

where a dot above a variable indicates the first derivative with respect to time, and two dots represent the second derivative. The following parameters are introduced:

$u_{1,stat} = \frac{F_0}{k_1}$ static deflection due to the amplitude of exciting force [m]

$\omega_1 = \sqrt{\frac{k_1}{m_1}}$ natural angular frequency of the main system [rad/s]

$\omega_E = \sqrt{\frac{k_2}{m_2}}$ natural angular frequency of TMD [rad/s]

$\lambda = \max|u_2 - u_1|$ maximum relative displacement between the main system and TMD [m]

From the particular solution of the differential equations (1) and (2), the maximum displacement of the main system can be expressed. This value must be minimized to optimize the system's performance and reduce vibrations effectively.

$$u^2{}_{1,max} = u^2{}_{1,stat} \frac{(\beta^2-\alpha^2)^2}{4\xi^2\beta^2(\beta^2-1+\mu\beta^2)^2+[\mu\alpha^2\beta^2-(\beta^2-1)(\beta^2-\alpha^2)]^2} \tag{3}$$

where the dimensionless parameters are:

$\alpha = \frac{\omega_E}{\omega_1}$ angular frequency ratio,

$\beta = \frac{\omega}{\omega_1}$ ratio between the frequency of excitation force and the natural frequency,

$\mu = \frac{m_2}{m_1}$ mass ratio between TMD and the main system,

$\xi = \frac{c}{2m_2\omega_E}$ TMD damping ratio.

An important aspect of the TMD design involves determining the relative displacement between the main system and the sprung damped mass. While precise determination is relatively difficult, this quantity can be verified through a dynamic STEP-BY-STEP calculation. Alternatively, an approximation of this quantity can be obtained using the following formula:

$$\left(\frac{\lambda}{u_{1,stat}}\right)^2 = \frac{u_1}{u_{1,stat}} \frac{1}{2\xi\mu\beta} \tag{4}$$

4. Optimal design of tuned mass damper

Each critical part (Fig. 1) is solved separately. Due to space limitations, only the result for part C) – the container platform – is presented here. The design values of the TMD constructed under the container platform are summarized in Fig. 4a). The efficiency of this TMD is expressed as the relationship between the ratio of the maximum dynamic displacement to the static displacement $abs(u_{1,max/u_{1,stat}})$ and the parameter β, which represents the dimensionless frequency of the applied load. This is depicted in Fig. 4b).

The test results for the maximum accelerations before the application of the TMD are shown in Fig. 5. It is expected that, with the TMD, the maximum acceleration can be reduced by a factor of approximately 0.4. The numerical results, which align closely with the test data, were also calculated. However, due to space constraints, these results are not presented in detail here.

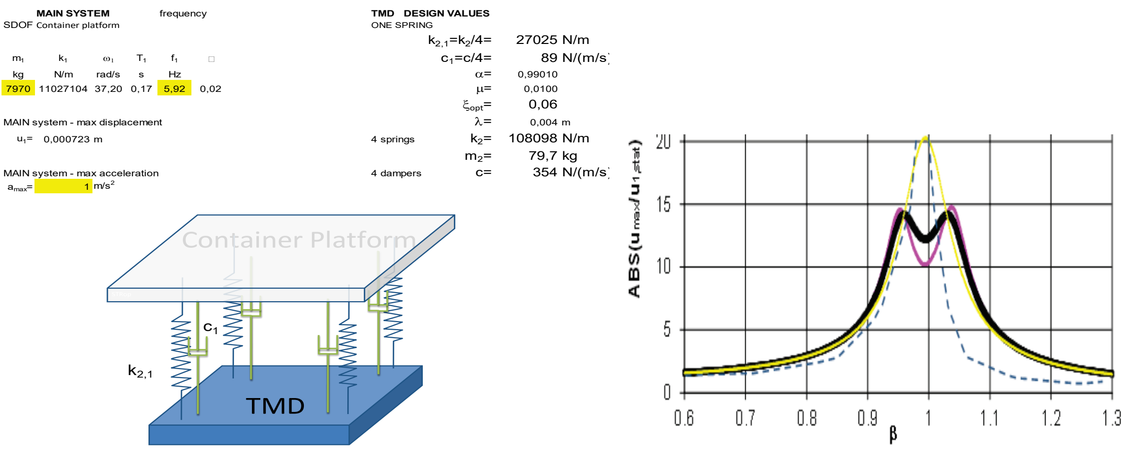

a) b)

Fig. 4: TMD under container platform, a) design values, b) efficiency with respect of load frequency.

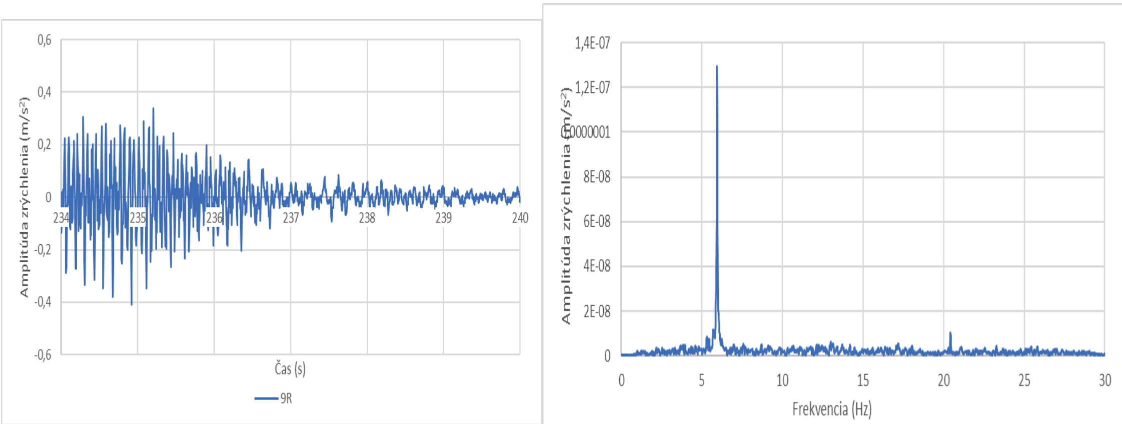

a) b)

Fig. 5: Test values of vertical vibrations on container platform
a) Acceleration versus time b) Acceleration amplitude spectra (FFT)

5. Conclusions

The first part of the paper focuses on the process of creating a digital twin of an industrial building. In-situ tests were conducted to determine the dynamic characteristics of the building, which were then compared with numerical analyses performed using the FEM method. Calibration was necessary to obtain accurate values for frequencies and eigenmodes in the analysis. Non-structural components had to be considered, as omitting them resulted in insufficiently precise results. Additionally, the process of designing an optimized TMD for the container platform was discussed. Three crucial damper parameters were determined: stiffness, damping, and the relative displacement between the main system and the TMD.

Acknowledgement

The authors would like to express their sincere gratitude to the Slovak Research and Development Agency (SRDA) for supporting and providing grant from research program APVV-22-0431 and for all support in frame of the project VEGA 1/0230/22.

References

Clough, R. W. and Penzien, J. (1993). *Dynamics of Structures* (2nd ed.). New York, NY: McGraw-Hill, 768.

Pacht, H. and Flesch, R. (1993). *Baudynamik - praxisgerecht*. Gütersloh, Germany: Bauverlag BV., 543, pp. 251-262.

Sarwar, W. and Sarwar, R. (2019) Vibration Control Devices for Building Structures and Installation Approach: A review. *Civil and Environmental Engineering Reports*, 29(2), pp. 74-100.